

*Short Communication*

## **Micro-arc Oxidation Coating Formed on Anodized Aluminum Surface under Different Pulse Frequencies**

Xuping Zhao, Dan Liu, Jieqin Lu, Guoying Wei\*

College of Materials Science & Engineering, China Jiliang University, Hang Zhou

\*E-mail: [guoyingwei@sina.com](mailto:guoyingwei@sina.com)

*Received:* 17 March 2017 / *Accepted:* 19 June 2017 / *Published:* 13 August 2017

---

The microstructure and corrosion behavior of the micro-arc oxidation (MAO) coating formed on the surface of anodization film under different pulse frequencies have been investigated. Microstructure of the coatings were examined by scanning electron microscopy (SEM), energy-dispersive spectroscopy (EDS) and X-ray diffractometer (XRD). Corrosion resistance of anodized coatings were evaluated by potentiodynamic polarization. The results reveal that the coating surface is more compact and the corrosion resistance is better with corrosion current one order of magnitude lower than coatings at lower frequencies. The surface roughness and hardness increased with the pulse frequencies. Al peaks decreased with the pulse frequency, indicating that more and more compact structure existed in the coatings.

---

**Keywords:** aluminum; anodization; micro-arc oxidation; pulse frequency

### **1. INTRODUCTION**

Aluminum alloy with light weight, high strength and excellent comprehensive performance has been widely used in various industrial fields. Still it also features a low surface hardness, poor wear resistance and weak corrosion resistance and etc. Therefore, the surface modification treatments such as anodic oxidation, chemical conversion coatings, ion implantation and laser processing are often adopted to improve the usage performance[1]. Anodization is a very common method for preparing the anodic oxide film. As a widely used technology, anodic oxidation is characterized with lower energy consumption and good appearance. However, the hardness and anticorrosion performance of the oxidation film treated with anodic oxidation technology is not very satisfying. Micro-arc oxidation, as a environment-friendly technology, prepares ceramic coatings with high corrosion resistance, wear resistance and better hardness[2]. In Meng[3] *Anodization for 2024 Al Alloy from Sulfuric-Citric Acid*

and Anticorrosion Performance of Anodization Films, the anodized coatings they made for 30min is about 10 $\mu$ m, at an oxidation voltage of 16V. In Shen[4] *Microstructure and corrosion behavior of micro-arc oxidation coating on 6061 aluminum alloy pre-treated by high-temperature oxidation*, with the MAO process under a constant current density of 4.4 A/dm<sup>2</sup> after 5 min MAO treatment, the thicknesses is 10-23  $\mu$ m. The MAO coatings they made on the surface of Al alloys were prepared for 30 min by MAO at different ratio of anodic and cathodic currents. The thickness of all the MAO coatings were about 30-40 $\mu$ m, and the hardness of the coatings prepared for 90 min were about 1200 HV. In the previous work of the authors[5-9], *The effect of pulse frequency on the electrochemical properties of micro arc oxidation coatings formed on magnesium alloy*, frequency is known to have strong effects on the MAO process under pulse power supply, so it is significant to combine anodic oxidation technology featuring lower energy consumption and micro-arc oxidation featuring optimal anticorrosion and hardness performance to obtain aluminum oxidation films.

In our work, both anodic oxidation and MAO method were applied to get a double-layer coating, which combines the advantages of the two methods. From the view of industrialization, it is better to prepare the same aluminum oxidized films under the condition of lower energy consumption. The effect of pulse frequency on the electrochemical properties of micro arc oxidation coatings formed on anodized aluminum is investigated, and the micro arc oxidation film has formed on the surface of anodization film under different frequencies.

## 2. MATERIALS AND METHODS

### 2.1. Material

The material used is 6061 aluminum alloy. The major alloying elements are given in Table 1. The specimens, 6cm $\times$ 2cm $\times$ 5mm in dimensions, were used as a substrate.

**Table 1.** Alloying elements

Alloying elements	Mg	Si	Fe	Mn	Cu	Cr	Zn	Ti
at%	0.8~1.2	0.4~0.8	$\leq$ 0.70	$\leq$ 0.15	0.15~0.40	0.04~0.35	$\leq$ 0.25	$\leq$ 0.15

### 2.2. Surface modification process

The aluminum alloy was polished with abrasive paper, then went through ultrasonic degreasing treatment in acetone. Activation was conducted in 0.5 mol/L nitric acid for 1 min after etching in a 2.5 mol/L NaOH solution at 80 $^{\circ}$ C for 30 s. Anodizing solution was composed of citric acid (153.6 g/L) and 8 ml/L sulfuric acid (98 %) with voltage of 16 V, temperature of 37 $^{\circ}$ C and the anodizing time of 40 min. The electrolyte of MAO consisted of Na<sub>2</sub>SiO<sub>3</sub> 20 g/L, 10 g/L Na<sub>3</sub>PO<sub>4</sub> and current density was

kept at less than  $5 \text{ A/dm}^2$ . Experiment temperature and duration were controlled at  $35^\circ\text{C}$  and 30 min respectively.

### 2.3. Electrochemical tests

Potentiodynamic polarization was carried out in a 3.5 wt.% NaCl solution, which is used as the corrosive media. Scanning rate of potentiodynamic polarization measurements is  $1\text{ mV/s}$ [10].

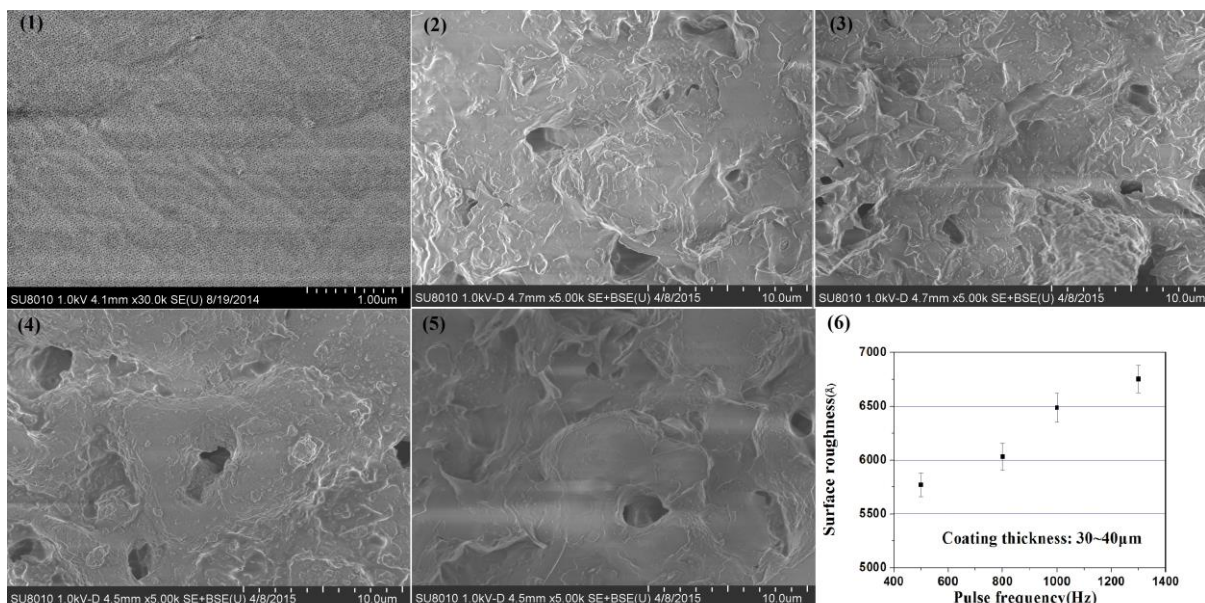
### 2.4. Microstructure tests

Surface morphologies and cross-morphologies of the coating were examined with field-emission scanning electron microscope (FESEM, SU8010) at an accelerating voltage of 20 kV. Thickness and component of films was measured by EDXRF spectrometer (EDX 1800B). The microstructural analysis of the coating was carried out using an X-ray diffractometer (DX-2700). Hardness was measured by microhardness tester (HV-1000).

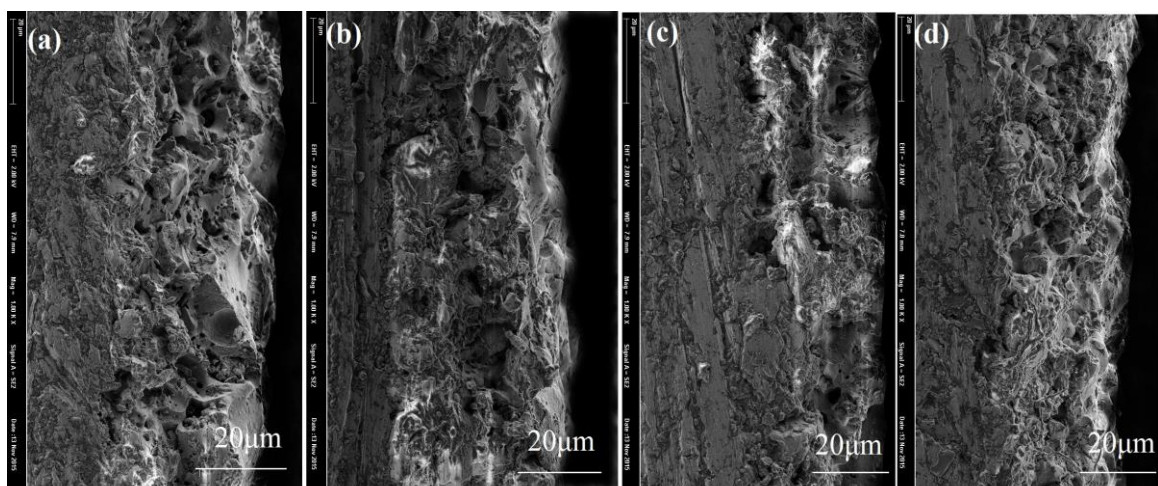
## 3. RESULTS AND DISCUSSION

Fig.1 illustrates the surface morphologies of the MAO coatings prepared under different pulse frequencies. The MAO coatings on the surface of anodization film were prepared for 20 min by MAO under different pulse frequencies. Fig.1 clearly indicates the oxidizing material in the form of pancakes distributing all over the surface at the coatings. All the coatings were compact, the pancake oxidizing material and crack-like structure have been observed. The pancake oxidizing material is rapidly solidified around the discharge channels. Some pancakes are solidified around the discharge channel. It is also obvious that the number of such pancakes decreases with the pulse frequencies. The pancake oxidizing material vanishes absolutely under 1300 Hz[11].

As observed from the morphology of the MAO coatings obtained at different pulse frequencies, the pore size is smaller and the surface is more compact at frequency of 1300 Hz as compared with the coating under other frequencies. The smaller micro-pore size and compact coating surface may facilitate the corrosion resistance of the MAO coatings. The differences in the micro-pore sizes in the four kinds of coatings can be attributed to the differences in the intensity of energy under these processing conditions. It was obvious that the surface roughness of the MAO coatings with similar thickness decreased when the pulse frequency increased. The change of the surface roughness was closely related to the surface morphologies of the coatings, especially the presence of the micro-pores. The larger the pancakes on the coating surface, the higher the surface roughness was obtained[12].



**Figure 1.** Surface morphology of micro-arc oxidation coatings formed on the surface of anodization film under different frequencies: (1) anodization film anodised under 16V at 37°C for 40min; (2) 500Hz; (3) 800Hz; (4) 1000Hz; (5) 1300Hz. (6) surface roughness of different pulse frequencies under the condition of the current density was kept at less than 5 A/dm<sup>2</sup>; T=35°C; t=30min.



**Figure 2.** Cross-sectional SEM micrographs and EDS line scan analysis of the MAO samples under different frequencies: (a) 500Hz; (b) 800Hz; (c) 1000Hz; (d) 1300Hz which the current density was kept at less than 5 A/dm<sup>2</sup>; T=35°C; t=30min.

Cross-sectional SEM micrographs of the MAO samples under different frequencies are shown in Fig.2. It can be found that all coatings well adhered to the substrate. Coatings of the MAO samples that were treated at 500Hz exhibited a highly porous nature with a coating thickness of about 35 µm. As the pulse frequencies increased, the coatings became thicker with more uniform surface and less porosity. The MAO coating (Fig.2) exhibits two distinct layer structures: a thin and dense layer at the

substrate interface, and a much thicker porous outer layer. On MAO samples, the interface between the micro arc oxidation film and the anodization film was not smooth. It could be the combined result of a rough starting surface. As shown in Fig.2 (a-d), it is obvious that the layer became thicker and denser when the pulse frequency increased[13-14].

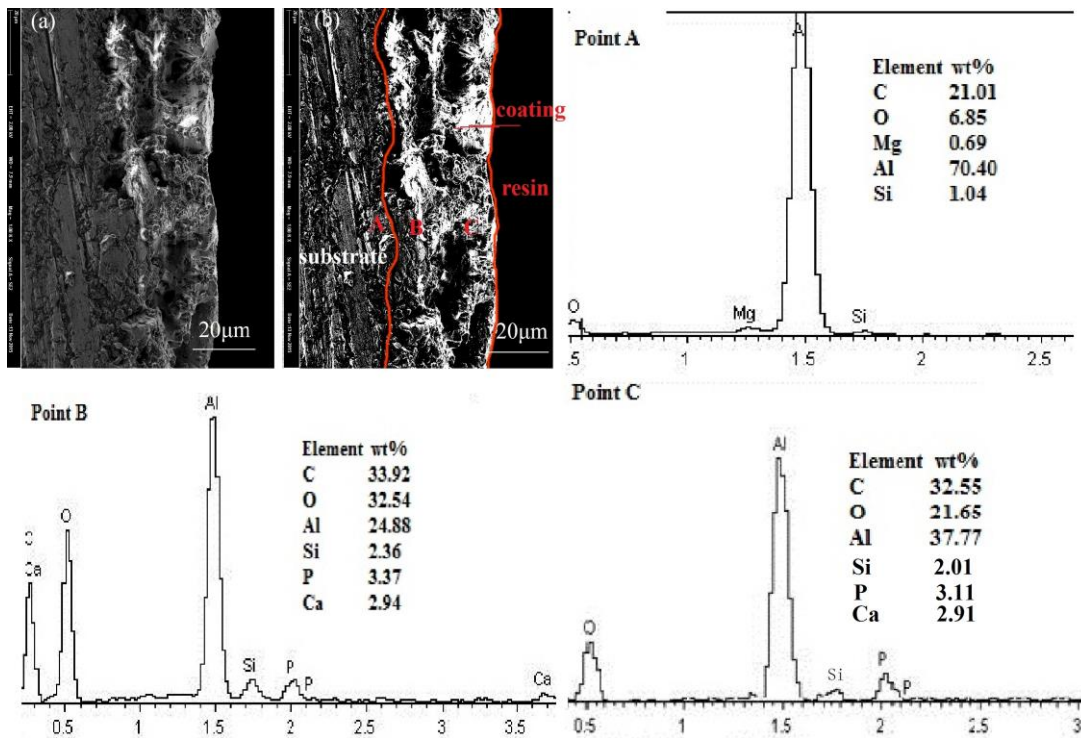


**Figure 3.** Cross-sectional SEM micrographs and EDS line scan analysis of the MAO samples under 500Hz which the current density was kept at less than 5 A/dm<sup>2</sup>; T=35°C; t=30min.

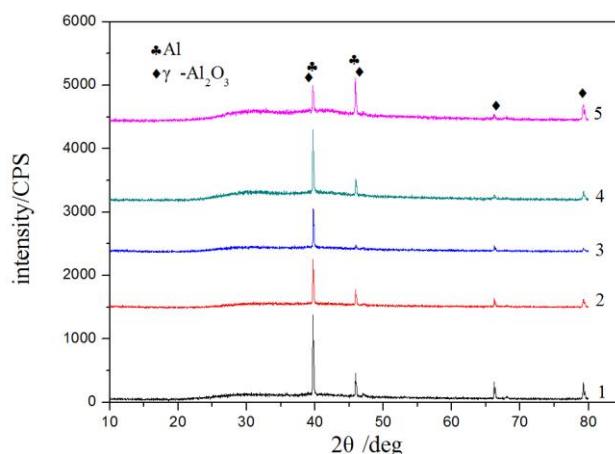


**Figure 4.** XRD pattern of micro arc oxidation film formed on the surface of anodization film under different frequencies: (1) anodization film anodised under 16V at 37°C for 40min; ; (2) 500Hz; (3) 800Hz; (4) 1000Hz; (5) 1300Hz under the condition of the current density was kept at less than 5 A/dm<sup>2</sup>; T=35°C; t=30min.

In order to further understand the growth patterns of the MAO coating, the morphology of cross-section of the MAO coatings were investigated by a magnified image(Fig.3(a and b)). Fig.3 shows the morphologies and distributions of elements Al, O, Si and Mg on the cross-section of the coating (Fig.3.b (point A, B and C)). It was found that the silicate content was decreasing on the point A, B and C. The coatings contain Si at 1.04, 2.36 and 0 % on the point A, B and C, respectively. This confirms the effective participation of  $\text{SiO}_4^{2-}$  ions at the initial stage of the MAO process, which is again attributed to the relative longer pulse-on-time[15].

Fig.4 shows the phases of MAO samples at four different pulse frequencies. The characteristic peaks corresponded to  $\gamma\text{-Al}_2\text{O}_3$  and Al can be defined as the patterns for all the specimens. The diffraction peaks of Al were aroused from the Al alloy substrate. Therefore, it can be deduced that the aluminum oxides in the MAO coatings was mainly crystalline  $\gamma\text{-Al}_2\text{O}_3$ .  $\gamma\text{-Al}_2\text{O}_3$  is known as a metastable phase of aluminum oxide, is formed at lower temperatures and tends to transform to  $\alpha\text{-Al}_2\text{O}_3$  at higher temperatures. Moreover, rapid cooling of molten oxide when in contact with the cold electrolyte during MAO process leads to the generation of  $\gamma\text{-Al}_2\text{O}_3$  phase on the surface of the oxide coating.

The intensity of Al peaks changed with different pulse frequencies. The intensity of Al peaks for the contrast sample(1) was relatively stronger, suggesting a more porous coating structure which was easy for X-rays to penetrate through the MAO coatings and get to the Al substrates. For the coatings 2, 3, 4 and 5, the intensity of Al peaks decreased with the pulse frequency, indicating that more and more compact structure existed in the coatings. Therefore, the results of XRD analysis further confirmed that the coatings presented a more compact structure with the increase of pulse frequency[16-17].

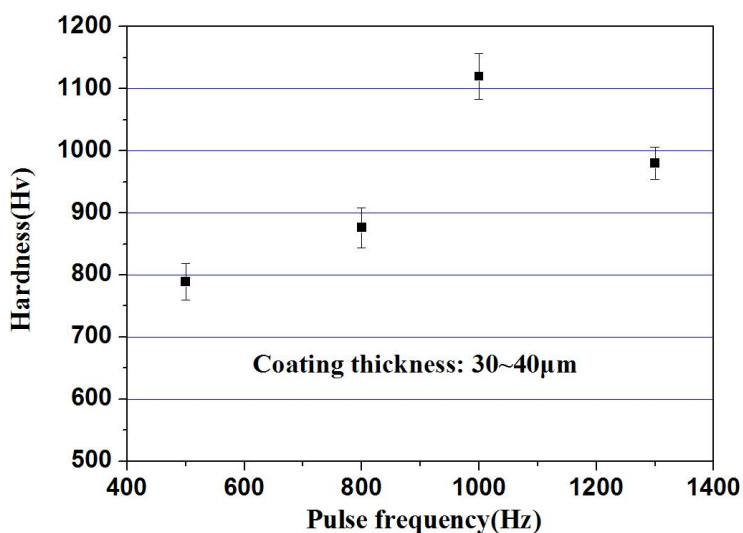


**Figure 5.** Influence of pulse frequency on surface hardness which the thickness of the coatings are similar(30~40 $\mu\text{m}$ )

Growth mechanism of oxide film is mainly decided by single pulse discharge energy. When the current density and duty ration were fixed, with the increase of pulse frequency, discharge time and pulse energy is not adequate. Therefore, molten oxide produced by single pulse could be relatively

uniform to form denser coatings. The hardness of the MAO coatings with similar thickness formed under different pulse frequencies is shown in Fig.5. It could also be noted that the hardness decreased remarkably under the frequency of 500 Hz. The hardness of ceramic coatings is measured six times respectively for getting the average value. The hardness increased with the increase of pulse frequency related to the results of XRD analysis, which confirmed that the coatings exhibited a more compact structure with the increase of pulse frequency[18].

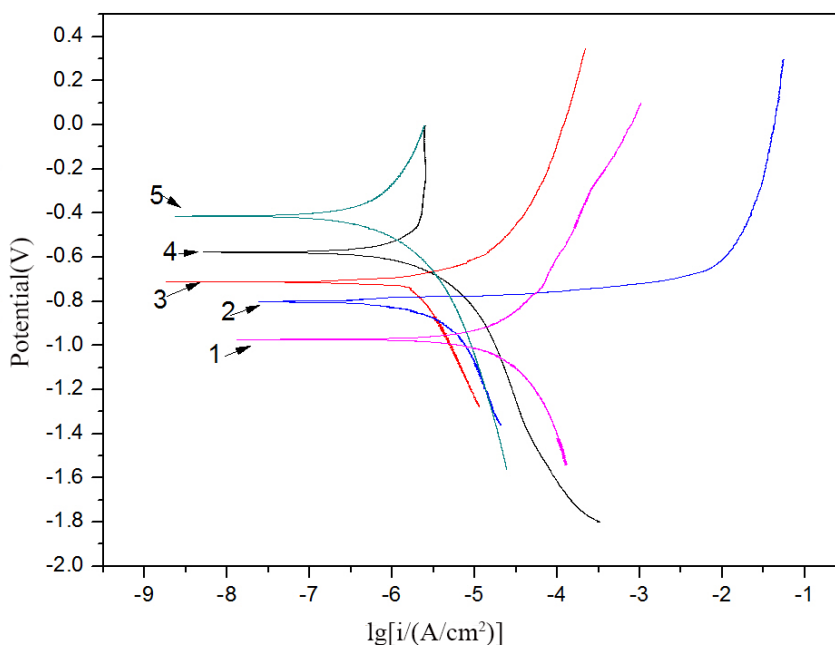


**Figure 6.** Polarization curves of micro arc oxidation film formed on the surface of anodization film under different frequencies (1) anodization film; (2)500Hz; (3)800Hz; (4)1000Hz; (5)1300Hz. after 20 min of immersion in a 3.5 wt.% NaCl solution. Temperature: 298K. Scan rate: 1mv/s.

**Table 2.** Corrosion parameters of microarc oxidation film formed on the surface of anodization film under different frequencies

Frequency	$E_{corr}(V)$	$i_{corr}$ ( $A/cm^2$ )	$\beta_c$ V/decade	$\beta_a$ V/decade
anodization film	-0.98	$1.62 \times 10^{-7}$	0.12	-0.10
500Hz	-0.82	$3.21 \times 10^{-7}$	0.06	-0.18
800Hz	-0.71	$4.05 \times 10^{-7}$	0.13	-0.07
1000Hz	-0.62	$4.17 \times 10^{-7}$	0.2	-0.17
1300Hz	-0.41	$1.69 \times 10^{-6}$	0.19	-0.28

The corrosion resistance properties of the MAO coatings prepared at four different frequencies were measured by potentiodynamic polarization test in a 3.5wt.% NaCl solution, as shown in Fig.6. More positive corrosion potential and/or low corrosion current indicates good corrosion resistance. The corrosion potential is more positive under the higher pulse frequency of 1300Hz. The corrosion resistance parameters indicated that the corrosion resistance of MAO coatings decreased with the pulse

frequency increased. Appropriate frequency of 1300Hz is beneficial for the coating anticorrosion performance, compared with the lower pulse frequencies. Corrosion potential of anodized film is -1.0V vs. Ag/AgCl (curve 1 in Fig. 6). The Corrosion parameters of micro arc oxidation film formed on the surface of anodization film under different frequencies are shown in Table 2. Corrosion potentials of micro arc oxidation film formed on the surface of anodization film under conditions of 500Hz~1300Hz are -0.82V, -0.71V, -0.62V and -0.41V, respectively. What's more, when the frequency are 500-1000Hz, the corrosion current density are the same magnitude ( $3.21 \times 10^{-7} \text{A/cm}^2$ ,  $4.05 \times 10^{-7} \text{A/cm}^2$ ,  $4.17 \times 10^{-7} \text{A/cm}^2$ ), with the frequency further increasing, the corrosion current density decreased ( $1.69 \times 10^{-6} \text{A/cm}^2$ ). It was expected that the corrosion resistance would be improved considerably, since it shows more positive corrosion potential and more negative corrosion current as the pulse increases. With the increase of pulse frequency, pore size of the oxide film gradually decreases to reduce the possibility of contact with corrosion solution and improve anticorrosion performance[19].

#### 4. CONCLUSIONS

Micro-arc oxidation (MAO) coating formed on the surface of anodization film under different pulse frequencies. Effects of different pulse frequencies on surface morphology, film thickness, hardness and anticorrosion performance of films were investigated in the paper. The conclusions are as following:

The pulse frequency has significant impact on the coating performance when the pulse frequencies decrease from 1300Hz to 500Hz. At higher frequency of 1300Hz, the coating surface is more compact and the corrosion resistance is better with corrosion current one order of magnitude lower than coatings at other lower frequencies, and lower corrosion resistance impedance. The hardness increased with the increase of pulse frequency related to the results of XRD analysis. The differences in the micro-pore sizes in the four kinds of coatings can be attributed to the differences in the intensity of energy under these processing conditions. All coatings well adhered to the substrate. As the pulse frequencies increased, the coatings became thicker with more uniform surface and less porosity.

#### ACKNOWLEDGEMENT

This research was supported by the National Natural Science Foundation (No. 51471156), Zhejiang Xinmiao Talents Program(No. 2016R409038) and International Science and Technology cooperation Program of China (No. 2011DFA52400).

#### References

1. D. Babilas, E. Urbanczyk, M. Sowa, A. Maciej, D.M. Korotin, I.S. Zhidkov, M. Basiaga, M. Krok-Borkowicz, L. Szyk-Warszynska, E. Pamula, E.Z. Kurmaev, S.O. Cholakh and W. Simka, *Electrochim. Acta*, 205 (2016) 256.
2. J. G. Yun, E.C. Kim and K. H. Kim. *Korean J. Metal. Mater.*, 54 (2016)1.



3. X. F. Meng, G.Y. Wei, H. L. Ge, Y.D.Yu , Y. Cao and H. Dettinger, *Int. J. Electrochem. Sci.*, 8 (2013) 10660.
4. D.J. Shen, G. L. Li, C.H. Guo, J. Zou, J.R. Cai, D. Lei, H.J. Ma and F.F. Liu, *Appl. Surf. Sci.*, 287 (2013) 451.
5. X. Song, J. Lu, X. Yin, J. Jiang and J. Wang. *J. Magn. Alloys*, 1 (2013) 318.
6. J.H. Wang, M.H. Du, F.Z. Han, J. Yang, *Appl. Surf. Sci.*, 292 (2014) 658.
7. D.J. Shen, J. R. Cai, G. L. Li, D. L. He, L. L. Wu, H. J. Ma, Y. H. Xia, H. Chen and Y.Q. Yang, *Vacuum*, 99 (2014) 143.
8. Y. Yürektürk, F. Muhaffel and M. Baydoğan, *Surf. Coat. Technol.*, 269 (2015) 83.
9. X. Y. Lu, X.G. Feng, Y. Zuo, C. B. Zheng, S. Lu and L. Xu, *Surf. Coat. Technol.*, 270 (2015) 227.
10. Q. B. Li, L.G. Jun, B.X. Liu, Z.J. Peng and Q. Wang, *Appl. Surf. Sci.*, 297 (2014) 176.
11. W.J. Zhu, Y. J. Fang, H.D. Zheng, G.X. Tan, H.M. Cheng and C.Y. Ning, *Thin Solid Films*, 544 (2013) 79.
12. X. Chen, D. L. Yu and L. Cao. *Mater. Res. Bull.*, 57 (2014)116.
13. F. Bayata, M. Ürgen, *J. Alloys Compd.*, 646 (2015) 719.
14. Y. Yang and L.L. Zhou. *J. Mater. Sci. Technol.*, 30 (2014) 1251.
15. C.S. Chi, J. H. Lee, I. Kim and H. J. Oh. *J. Mater. Sci. Technol.*, 31 (2015) 751.
16. W.P. Li, Z.Y. Qian, X. H. Liu, L.Q. Zhu and H.C. Liu. *Appl. Surf. Sci.*, 356 (2015) 581.
17. Y. F. Ge, B. L. Jiang, M. Liu, C.J. Wang and W.N. Shen. *J. Magn. Alloys*, 2 (2014) 309.
18. K. Korkmaz. *Surf. Coat. Technol.*, 272 (2015) 72.
19. [20] C. Fares, L. Hemmouche, M. A. Belouchrani, A. Amrouche, D. Chicot and E.S. Puchi-Cabrera, *Mater. Des.*, 86 (2015) 723.

© 2017 The Authors. Published by ESG ([www.electrochemsci.org](http://www.electrochemsci.org)). This article is an open access article distributed under the terms and conditions of the Creative Commons Attribution license (<http://creativecommons.org/licenses/by/4.0/>).